Iron isotope and trace metal records of iron cycling in the proto-North Atlantic during the Cenomanian-Turonian oceanic anoxic event (OAE-2)

Jeremy D. Owens,[1] Timothy W. Lyons,[1] Xiaona Li,[2] Kenneth G. Macleod,[3] Gwenyth Gordon,[4] Marcel M. M. Kuypers,[5] Ariel Anbar,[4,6] Wolfgang Kuhnt,[7] and Silke Severmann[2]

Received 29 March 2012; revised 10 July 2012; accepted 14 July 2012; published 29 August 2012.

[1] The global carbon cycle during the mid-Cretaceous (~125–88 million years ago, Ma) experienced numerous major perturbations linked to increased organic carbon burial under widespread, possibly basin-scale oxygen deficiency and episodes of euxinia (anoxic and H_2S-containing). The largest of these episodes, the Cenomanian-Turonian boundary event (ca. 93.5 Ma), or oceanic anoxic event (OAE) 2, was marked by pervasive deposition of organic-rich, laminated black shales in deep waters and in some cases across continental shelves. This deposition is recorded in a pronounced positive carbon isotope excursion seen ubiquitously in carbonates and organic matter. Enrichments of redox-sensitive, often bioessential trace metals, including Fe and Mo, indicate major shifts in their biogeochemical cycles under reducing conditions that may be linked to changes in primary production. Iron enrichments and bulk Fe isotope compositions track the sources and sinks of Fe in the proto-North Atlantic at seven localities marked by diverse depositional conditions. Included are an ancestral mid-ocean ridge and euxinic, intermittently euxinic, and oxic settings across varying paleodepths throughout the basin. These data yield evidence for a reactive Fe shuttle that likely delivered Fe from the shallow shelf to the deep ocean basin, as well as (1) hydrothermal sources enhanced by accelerated seafloor spreading or emplacement of large igneous province(s) and (2) local-scale Fe remobilization within the sediment column. This study, the first to explore Fe cycling and enrichment patterns on an ocean scale using iron isotope data, demonstrates the complex processes operating on this scale that can mask simple source-sink relationships. The data imply that the proto-North Atlantic received elevated Fe inputs from several sources (e.g., hydrothermal, shuttle and detrital inputs) and that the redox state of the basin was not exclusively euxinic, suggesting previously unknown heterogeneity in depositional conditions and biogeochemical cycling within those settings during OAE-2.

Citation: Owens, J. D., T. W. Lyons, X. Li, K. G. Macleod, G. Gordon, M. M. M. Kuypers, A. Anbar, W. Kuhnt, and S. Severmann (2012), Iron isotope and trace metal records of iron cycling in the proto-North Atlantic during the Cenomanian-Turonian oceanic anoxic event (OAE-2), *Paleoceanography*, *27*, PA3223, doi:10.1029/2012PA002328.

1. Introduction

[2] The Late Cretaceous greenhouse interval peaked during the late Cenomanian and early Turonian, and the Cenomanian-Turonian boundary coincides with a major perturbation of the global carbon cycle [*Scholle and Arthur*, 1980; *Schlanger et al.*, 1987; *Arthur et al.*, 1988] reflected in extensive deposition of laminated black shales. These

[1]Department of Earth Sciences, University of California, Riverside, California, USA.

Corresponding author: J. D. Owens, Department of Earth Sciences, University of California, 900 University Ave., Riverside, CA 92521, USA. (jowens@student.ucr.edu)

[2]Institute of Marine and Coastal Sciences, Rutgers, State University of New Jersey, New Brunswick, New Jersey, USA.
[3]Department of Geological Sciences, University of Missouri, Columbia, Missouri, USA.
[4]School of Earth and Space Exploration, Arizona State University, Tempe, Arizona, USA.
[5]Department of Biogeochemistry, Max Planck Institute for Marine Microbiology, Bremen, Germany.
[6]Department of Chemistry and Biochemistry, Arizona State University, Tempe, Arizona, USA.
[7]Universität Kiel, Institut für Geowissenschaften, Kiel, Germany.

perturbations resulted from either increased primary production [*Schlanger and Jenkyns*, 1976], enhanced organic matter preservation under oxygen-deficient depositional conditions [*Barron*, 1983; *Schlanger et al.*, 1987], or some combination of both. Associated with elevated temperatures [*Huber et al.*, 1995] and thus lower oxygen solubility, along with enhanced carbon delivery, the environmental conditions of the basinal proto-North Atlantic became anoxic and euxinic (with free H_2S in the water column) at a scale large enough to be termed an oceanic anoxic event or OAE [*Schlanger and Jenkyns*, 1976; *Jiménez Berrocoso et al.*, 2008; *Hetzel et al.*, 2009]. The result was a proliferation of organic-rich, laminated black shales in the deep basin and less commonly across continental shelves, particularly at sites along the tropical Atlantic shelf—i.e., the southern part of the proto-North Atlantic Basin. A sharp increase in organic matter burial is reflected in a global positive isotope excursion expressed in both organic and inorganic carbon across the basin [*Schlanger and Jenkyns*, 1976; *Arthur et al.*, 1988]. The prominent isotope excursion, particularly its expression in the organic record, is especially useful for correlating basin-wide stratigraphy in the absence of biostratigraphic controls at paleodepths greater than the carbonate compensation depth [*Kuhnt et al.*, 2005].

[3] A common model for the cause of OAE-2 calls upon the expansion of hydrothermal activity [*Sinton and Duncan*, 1997; *Jones and Jenkyns*, 2001; *Kuroda*, 2007; *Frijia and Parente*, 2008; *MacLeod et al.*, 2008; *Turgeon and Creaser*, 2008; *Adams et al.*, 2010], resulting in increased concentrations of hydrothermal Fe in the photic zone prior to the onset of the OAE and a concomitant increase in primary production [*Leckie et al.*, 2002; *Snow et al.*, 2005]. Studies of the modern ocean tell us that primary production over vast regions can be limited by the availability of Fe, an essential micronutrient [*Martin and Fitzwater*, 1988]. By analogy, hydrothermal Fe is hypothesized as a possible explanation for the increased organic carbon deposition that marks the OAE. The coincidence of the emplacement of the Caribbean large igneous province (LIP) with sedimentary trace metal enrichments [*Snow et al.*, 2005] and marked radiogenic isotope excursions for Nd [*Kuroda*, 2007; *Frijia and Parente*, 2008; *MacLeod et al.*, 2008] and non-radiogenic isotope excursions for Sr and Os [*Jones and Jenkyns*, 2001; *Turgeon and Creaser*, 2008] are consistent with a volcanogenic trigger for large-scale ocean anoxia. However, recent work suggests there is also a significant increase in continental weathering and/or detrital inputs during the event [*Jones and Jenkyns*, 2001; *Blättler et al.*, 2011], which may complicate these isotopic signals [as reviewed in *Jenkyns*, 2010].

[4] Importantly, Fe enrichments do not necessarily imply enhanced hydrothermal activity. Therefore, we need to investigate possible Fe sources in great detail. For example, enhanced remobilization of Fe from coastal sediments is an alternative model for the delivery of Fe to the open ocean during ocean-scale anoxia. Benthic Fe fluxes correlate positively with rates of organic matter oxidation until the onset of bacterial sulfate reduction, and bottom water oxygen concentrations are inversely proportional [*Elrod et al.*, 2004; *Severmann et al.*, 2010]. Consistent with a relationship to high availability of organic matter, modern oxygen minimum zones (OMZ) demonstrate elevated Fe concentrations in the water column [*Bruland et al.*, 2005; *Moffett et al.*, 2007; *Blain et al.*, 2008]. The expansion of oceanic anoxia thus provides a positive feedback for enhanced Fe supply from the continental shelf to the open ocean. The mechanistic underpinnings of this model have emerged from careful studies of the Black Sea, the modern world's largest euxinic basin, wherein diverse evidence points to net transport (shuttling) of reactive Fe from shallow oxic and suboxic shelf settings to deep euxinic waters (as reviewed in *Lyons and Severmann* [2006]). Detailed measurements and models have specifically fingerprinted and quantified net transport of reactive Fe from the shelf to the basin where it is captured through pyrite formation in the water column [*Canfield et al.*, 1996; *Wijsman et al.*, 2001; *Anderson and Raiswell*, 2004]. The shallow, organic carbon-lean, oxic-to-suboxic sites along the basin margin show correlative loss of Fe from the sediment pore waters and thus from the bulk sediments through reductive cycling in the absence of appreciable dissolved H_2S.

[5] Our goal is to evaluate the relative roles of basinal redox controls and increased volcanic activity in the enhanced delivery of Fe during the OAE. To better understand the origin of Fe enrichments we have investigated sections from seven different locations (Figure 1) representing continental shelf, continental rise, and deep abyssal plain settings spanning the Cenomanian-Turonian boundary and associated with clear independent records of OAE-2, such as $\delta^{13}C$ relationships. Most of the sites have previously been described to have enrichments in redox-sensitive trace metals such as Fe, Cu, Mo, and V [*Brumsack*, 1980; *Jiménez Berrocoso et al.*, 2008; *Hetzel et al.*, 2009; *van Bentum et al.*, 2009], and several sites show organic biomarker evidence for pervasive photic-zone euxinia prior to and throughout the OAE [*Sinninghe Damsté and Köster*, 1998; *Kuypers et al.*, 2002; *Pancost et al.*, 2004]. Here we couple Mo concentration data to our Fe analyses as an independent constraint on the local depositional redox conditions. We are using Fe concentrations and isotopes to understand the basin-wide Fe geochemistry in the proto-North Atlantic and specifically the pathways of Fe cycling, from source to sink. Included in this mix is the possible role of an iron "shuttle" analogous to that operating today in the Black Sea but on the scale of a large ocean basin. This is the first exploration of the shuttle model at such a scale and under the likely strong influence of hydrothermal contributions. Hydrothermal inputs may mask the shelf-to-basin shuttling of Fe that is perhaps more easily recognized in marginal marine basins and epicontinental seaways under a favorable source-to-sink mass balance.

2. Background: Iron Isotopes as a Source Tracer

[6] Elevated bulk iron (Fe_T) to aluminum (Al) ratios are a simple indicator of sedimentary Fe enrichment beyond the continental crustal average of ~0.5 [*Turekian and Wedepohl*, 1961; *Taylor and McLennan*, 1995] and are among the most dependable indicators of ancient redox conditions and Fe cycling in those settings [*Lyons and Severmann*, 2006; *Raiswell et al.*, 2008]. The differentiation of multiple Fe sources for the enrichment, however, requires additional proxies that can help refine our understanding of environmental conditions and the associated enrichment mechanism(s). Iron isotopes can be important tracers of Fe inputs in these studies because each potential source, in this case hydrothermal fluids

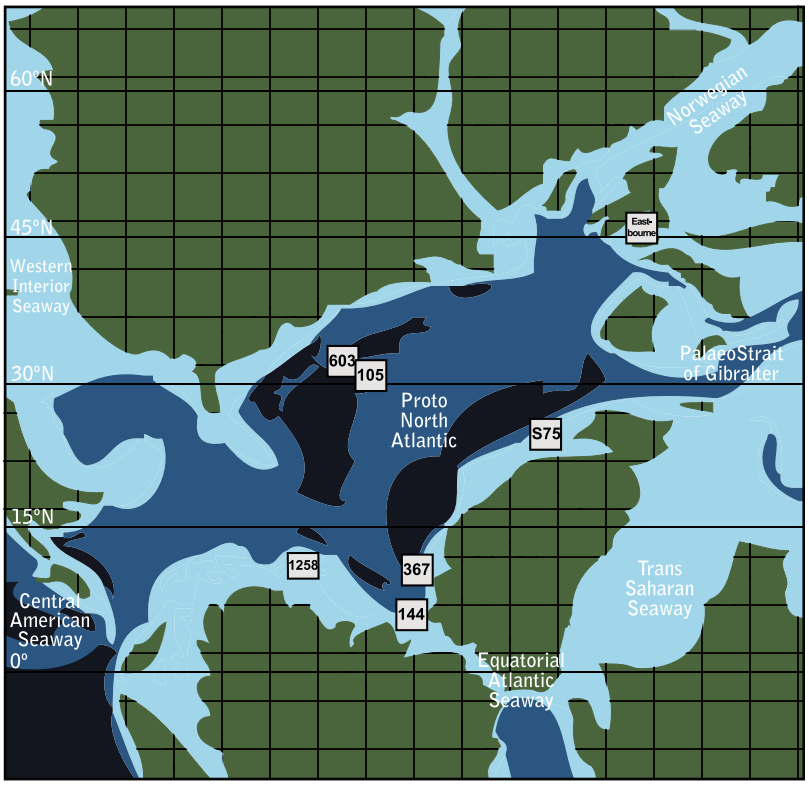

Figure 1. Sample location for the seven sections investigated within the proto-North Atlantic; paleogeography adapted from *Trabucho Alexandre et al.* [2010]. The blue gradient indicates estimated water depths with the lighter colors indicating shallower depths and greater depths marked with darker colors; the landmasses are shaded green and gridded.

versus diagenetic Fe released from (and remobilization within) sediments, should have distinct isotopic properties.

[7] The majority of hydrothermal fluids measured to date show only minimal deviation in their Fe isotope compositions (δ^{56}Fe, see below for further explanation) relative to average igneous rocks (~0.0‰ to −0.5‰) [*Sharma et al.*, 2001; *Beard et al.*, 2003; *Severmann et al.*, 2004]. Deviations from this value are typically only observed for lower temperature fluids, which have much lower Fe concentrations; therefore, it would be difficult for this source to significantly impact the isotopic geochemistry of the sediments. In the modern oxic ocean the isotopic compositions of freshly precipitated Fe in hydrothermal plumes suggest a complex picture as different mineral phases, such as pyrite and Fe oxides, that form upon mixing of hot fluids with cold seawater. However, despite the potential for isotopic fractionation during hydrothermal fluid entrainment into the bottom water, Fe isotope compositions of distal hydrothermal plume particles have been shown to span a relatively narrow range, with values approaching the fluid source [*Severmann et al.*, 2004; *Bennett et al.*, 2009]. The geologic record confirms that sediments with hydrothermally sourced Fe also span a narrow range in δ^{56}Fe values similar to modern hydrothermal fluids, but show a large range in Fe_T/Al ratios consistent with Fe enrichment [*Johnson et al.*, 2008; *Czaja et al.*, 2010; *Halverson et al.*, 2011]. Consequently, the Fe isotope composition of hydrothermally impacted sediments is relatively invariant, regardless of the degree of Fe enrichment. It is difficult to distinguish detrital inputs from hydrothermal contributions using Fe isotopes alone; however, the use of Fe_T/Al ratios helps us discern relative contributions —with detrital Fe_T/Al values of ~0.5 and hydrothermal values typically much greater than 0.5. An increase in detrital material via weathering patterns could add an additional complication because hydrothermal isotopic and enrichment signatures in a marginal environment can be diluted by enhanced continental delivery.

[8] The iron shuttle initiates with preferential release of isotopically light Fe during reduction of oxide phases coupled to diagenetic carbon remineralization beneath the oxic/suboxic shelfal bottom waters of the source region [*Severmann et al.*, 2006]. As a result, the residual bulk sedimentary Fe becomes preferentially depleted in total Fe and isotopically enriched with a positive δ^{56}Fe signature. The remobilized, shuttled light Fe is subsequently captured through water column pyrite formation in the euxinic basin [*Lyons*, 1997]. Iron capture in the sulfidic water column is near quantitative; such a mass balance implies that the isotopic composition of the precipitated Fe remains indistinguishable from the dissolved source. As a consequence, the sediments show increasingly light Fe isotope values with progressive Fe enrichments [*Lyons and Severmann*, 2006; *Severmann et al.*, 2008]. This pattern, specifically an inverse relationship between $\delta^{56}Fe_T$ and Fe_T/Al, can provide a robust fingerprint of Fe shuttling in ancient basins [*Czaja et al.*, 2010; *Duan et al.*, 2010]. However, the role and fingerprints of the shuttle on the scale of a deep ocean OAE

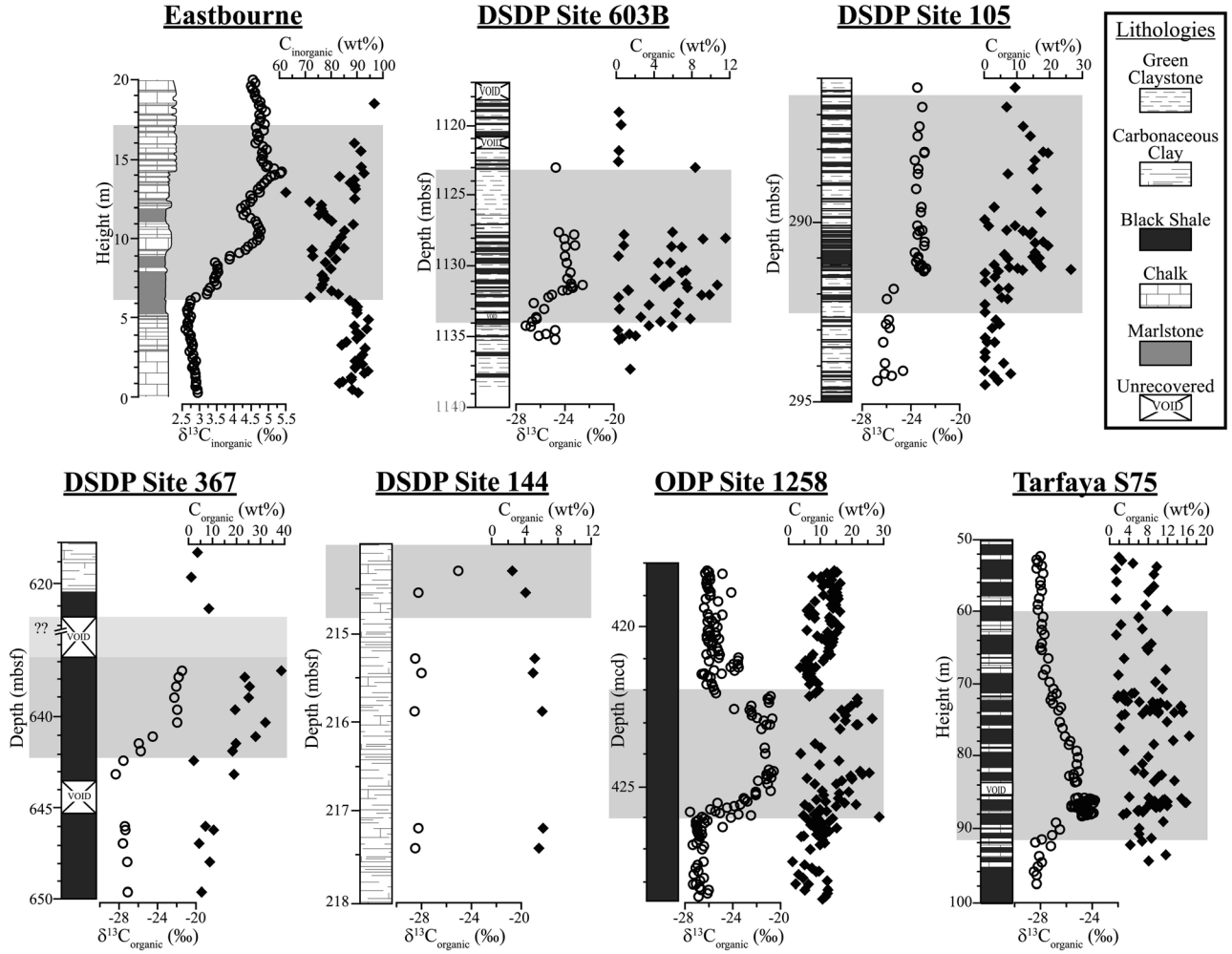

Figure 2. Lithostratigraphy and carbon isotope stratigraphy. The rapid positive shift in the $\delta^{13}C$ of organic carbon (open circle) denotes the excursion of OAE-2 (gray box), although the termination of the event is not always well defined. Total organic carbon is also plotted (black diamond). Note that the positive $\delta^{13}C$ shift at Eastbourne is represented in the data for inorganic carbon, with inorganic carbon concentrations also plotted. Eastbourne lithostratigraphy and carbon isotopes from *Tsikos et al.* [2004], DSDP 603B and DSDP 105 from *Kuypers et al.* [2004] with additional lithostratigraphy from *van Hinte et al.* [1987], DSDP 367 from *Kuypers et al.* [2002], ODP 1258 carbon isotopes from *Erbacher et al.* [2005] and lithostratigraphy from *Shipboard Scientific Party* [2004], Tarfaya S75 from *Kuhnt et al.* [2005].

are not well studied—a gap that motivated the approach taken here.

3. Sampling: Sites and Collection Protocols

[9] Here we present data from seven sample localities deposited under variable redox conditions. The sample locations were strategically selected with an eye toward wide spatial distribution in the proto-North Atlantic (Figure 1). Most of the samples used for this study were obtained from Deep Sea Drilling Project (DSDP) and Ocean Drilling Program (ODP) sample archives. Our existing sample collections (DSDP sites 105, 144, 367 and 603B and ODP site 1258 [*Berger and von Rad*, 1972; *Hayes et al.*, 1972; *Hollister et al.*, 1972; *van Hinte et al.*, 1987; *Thurow*, 1988; *Shipboard Scientific Party*, 2004]) were complemented with additional samples obtained from the core repository in Bremen, Germany, in 2008. Samples from Tarfaya core S75 were collected as part of the oil shale campaign undertaken by Shell International Exploration and Production [*Kuhnt et al.*, 1997], and the Eastbourne outcrop section was logged and sampled at the Gun Gardens locality in East Sussex, England. Three sites were located in the northern region of the proto-North Atlantic and four from the southern region (Figure 1).

[10] The Eastbourne locality from the northern proto-North Atlantic represents a shallow oxic shelf [*Paul et al.*, 1999; *Tsikos et al.*, 2004] with very low total organic carbon (TOC) content (Figure 2; TOC of 0.1 to 0.2 wt. %) and lithologies (Figure 2) dominated by bioturbated nannofossil (coccolithophore) calcareous ooze and clay [*Gale*, 1996; *Keller et al.*, 2001]. Despite fundamental differences in the

depositional environment of this oxic site relative to our other localities, carbonate-C and organic-C isotope records of OAE-2 are well correlated with those from the other sites (Figure 2).

[11] Two northern proto-North Atlantic sites, DSDP sites 603B and DSDP 105, have mixed lithologies that document fluctuating redox conditions. Deposition during the OAE at both sites is marked by alternating organic-poor green claystone (TOC ~1 wt. %) and organic-rich black shales (TOC up to 25 wt. %) (Figure 2) with consistently low carbonate abundance (<10 wt. %) [*Herbin et al.*, 1987], suggesting periodic anoxia/euxinia and possible orbital forcing of organic carbon deposition and associated depositional redox [*Kuypers et al.*, 2004]. The main distinction between these two sites is that 603B was under stronger influence of coastal oceanic processes, and the sediments are therefore distinctly hemipelagic [*Herbin et al.*, 1987]. The intermittence of the laminated, metal-enriched black shales, along with biomarker evidence [*Kuypers et al.*, 2004], suggests that this part of the North Atlantic was only periodically euxinic during the OAE. Consistent with this inferred redox-oscillation, the green claystones (Figure 2) are bioturbated and do not show enrichments of redox-sensitive metals, consistent with oxic conditions of deposition [*Kuypers et al.*, 2004]; this alternation occurs at very regular intervals (0.11–0.13 m), and the lithologies before and after the OAE at both sites are dominantly bioturbated organic-lean green claystones with some fine layers of organic-rich shales.

[12] Black shale deposition was particularly prominent in the southern portion of the proto-North Atlantic during the OAE [*Trabucho Alexandre et al.*, 2010]. Of the four sites from the southern part of the basin (Figure 1), DSDP site 367 near Cape Verde was the deepest, with a paleodepth of ~3700 m located on the abyssal plain in the vicinity of the ancestral mid-ocean ridge [*Kuypers et al.*, 2002]. Even before the onset of the OAE (as marked by the positive C-isotope excursion, Figure 2), sediments show pronounced lamination (Figure 2) [*Herbin et al.*, 1986] and high TOC contents that increase to exceptionally high values-of up to 40 wt. % during the event. Previously noted at this site was the appearance of isorenieratene and chlorobactene, sulfur-bound molecular fossils, produced by brown and green strains of phototrophic sulfur bacteria, indicating that euxinic conditions extended at least episodically into the photic zone during the OAE [*Kuypers et al.*, 2002].

[13] ODP site 1258 (all samples from core 1258A) from the Demerara Rise is marked by finely laminated black shales that extend before, during, and after OAE-2, with TOC contents reaching maximum values of 30 wt. % during the event. Previous records of Fe enrichment, the S isotope compositions, and prevalent lamination indicate persistent euxinia during the OAE at this site [*Hetzel et al.*, 2009] while a positive Nd isotope excursion [*MacLeod et al.*, 2008] may hint at hydrothermal contributions to the local bottom waters. The core depths [specifically meter core depth (MCD) below the seafloor] for data presented here for Fe and Mo were adjusted to correlate with the carbon isotope stratigraphy of *Erbacher et al.* [2005] using the method presented in the supplementary material of *MacLeod et al.* [2008].

[14] S75 from Tarfaya, Morocco, is a relatively shallow, shelfal site (<200 m paleo-water depth [*Kuhnt et al.*, 1997]) with high sedimentation rates exceeding 10 cm/kyr, making its accumulation rates for organic matter the world's highest known for the C/T transition. Sediments are comprised of organic rich (TOC up to 15 wt. %) dark laminated chalks and carbonate-diluted shales [*Kolonic et al.*, 2005] intercalated with non-laminated, lighter colored limestones (Figure 2). Isorenieratane abundance increases dramatically up section in a nearby core (Tarfaya S13) during the OAE, indicating photic zone euxinia, although there is a slight increase just before the OAE, and concentrations remain high slightly after the OAE [*Kuypers et al.*, 2002]. Previously, a similar Tarfaya site (section S57) was analyzed by *Jenkyns et al.* [2007] for Fe, C and N isotopes. Details are discussed below.

[15] Last, sediments at another open ocean site from the southern proto-North Atlantic, DSDP 144, were deposited at a relatively shallow paleodepth of ~1300 m on the ancestral mid-ocean ridge [*Berger and von Rad*, 1972], supporting the likelihood of high hydrothermal inputs at this site. Sediments consist of laminated carbonaceous limestone and calcareous clay with TOC contents reaching 30 wt. % during the OAE. Isorenieratane is present at this site, although the abundances are lower than those at site 367 [*Kuypers et al.*, 2002].

4. Analytical Methods

[16] Once inspected and cleaned, the samples were powdered using a trace metal-clean ceramic ball mill and ashed for 12 h at ~850°C to volatilize any organic material and sulfides. The samples were then weighed to determine loss on ignition, and 50–75 mg of ashed sample were digested by a standard three-acid sequential protocol using HNO_3/HCl/HF at ~150°C. All acids used were Aristar/trace metal clean. Fully digested samples were analyzed on an Agilent 7500ce ICP-MS (Inductively Coupled Plasma-Mass Spectrometer) using H_2 and He in the collision cell. Standard reference materials (SDO-1 and SCO-1 shales) were digested and analyzed with each set of extractions, and in all cases were within the accepted analytical error for all elements: Fe and Al had % errors of less than ±5, and Mo had an error of ±8, which is better than the certified value. We emphasize total Fe in this study because most of the cores have oxidized since collection, which precludes detailed speciation such as that of *Poulton and Canfield* [2005]. Fortunately, the depositional and diagenetic conditions of interest are well expressed in the Fe properties of the bulk sediment [*Lyons and Severmann*, 2006].

[17] Splits from the previously dissolved materials were used to measure the Fe isotope composition of the bulk sample ($\delta^{56}Fe_T$). To eliminate matrix effects, samples were purified using anion exchange resin (0.5 ml of Biorad AGMP-1 M) and a standard ion chromatography protocol for Fe separation [*Skulan et al.*, 2002; *Arnold et al.*, 2004]. Column yields were monitored before and after chromatographic purification using a modified ferrozine colorimetric method [*Stookey*, 1970; *Viollier et al.*, 2000] with UV-V is spectrophotmetry (λ = 562 nm). Samples with yields of 95% or better were dried down and diluted with 0.32 M HNO_3 for isotopic analysis.

[18] Isotopic compositions were measured on a Neptune Thermo Scientific MC-ICP-MS (Multiple Collector-Inductively Coupled Plasma-Mass Spectrometer) at Arizona State University using the methods described in *Arnold et al.* [2004]. The samples were run in a 0.32 M HNO_3 matrix at ~2–3 ppm

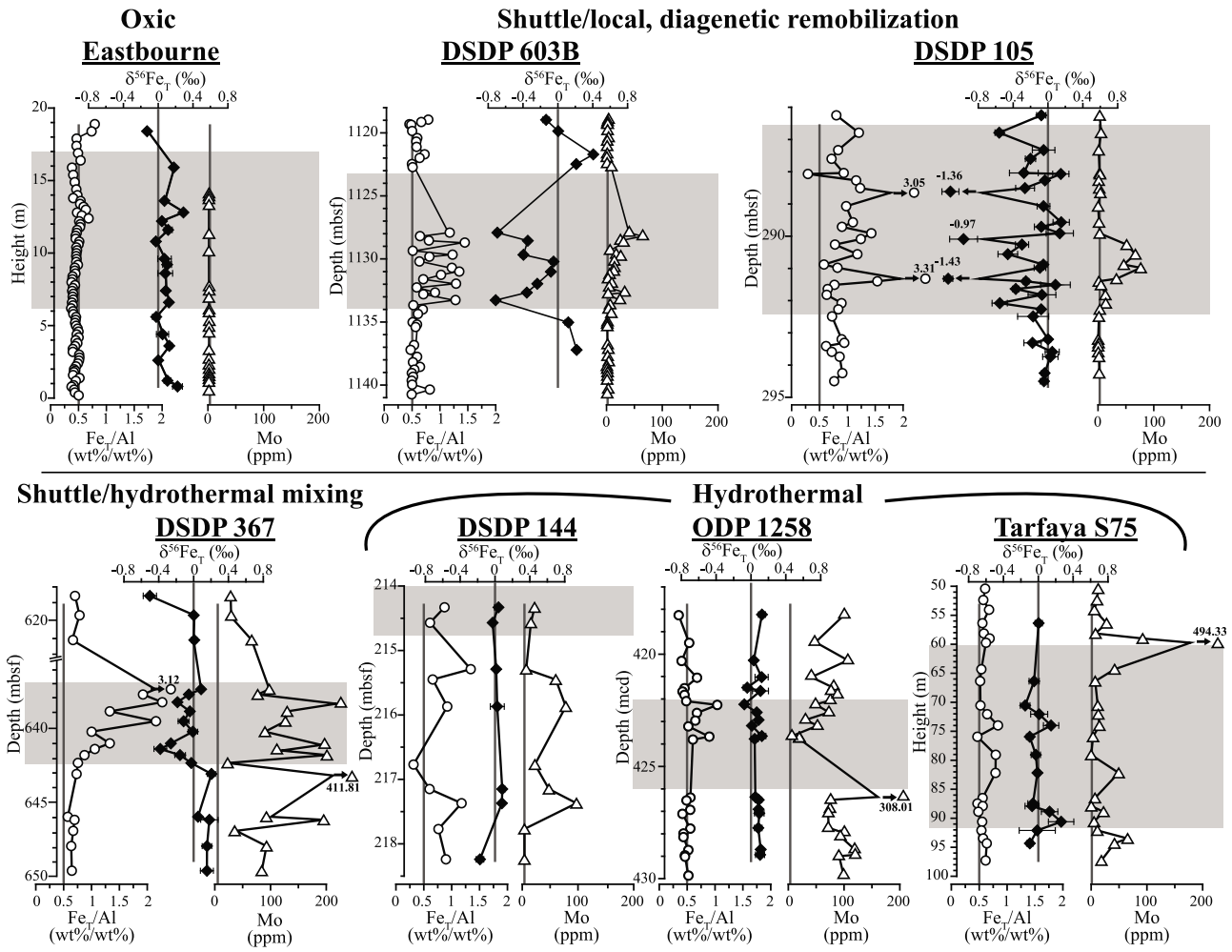

Figure 3. Detailed Fe and Mo data for each site plotted stratigraphically. The gray bar indicates the OAE as defined by the carbon isotope stratigraphy. The solid lines indicate the crustal average for each elemental concentration. The $\delta^{56}Fe_T$ data are shown with horizontal error bars (2 SD).

Fe concentration and spiked with equal proportion of Cu standard for mass bias correction. We measured the certified international reference material IRMM-014 as a bracketing standard between each sample as a further monitor for accurate mass bias correction. Corrected data are reported relative to average igneous rock using the standard delta notation [*Coplen*, 2011]:

$$\delta^{56}Fe(‰) = \left[\frac{\left(\left({}^{56}Fe/{}^{54}Fe\right)sample\right)}{\left(\left({}^{56}Fe/{}^{54}Fe\right)IgnRx\right)}\right] - 1$$

The measured Fe isotope composition of IRMM-014 is $\delta^{56}Fe_T$ −0.09‰ on this scale [*Beard et al.*, 2003] with a long-term internal precision of ±0.08‰ (2-STD).

5. Results and Discussion

[19] This study is the most comprehensive Fe isotope study to date of an OAE, although not the first Fe isotope data set for OAE-2 [*Jenkyns et al.*, 2007] or Cretaceous black shales [*Clayton et al.*, 2007]. The uniqueness of our study lies with our inclusion of extensive data for Fe and Mo concentrations and samples from diverse settings and depositional conditions spanning from before, during, and after the event (see Figure 3 and auxiliary material).[1] We begin our discussion by reconstructing paleoenvironmental conditions using Mo concentrations. These data provide an essential framework for interpreting the Fe-isotope and Fe_T/Al relationships and, specifically, for unraveling Fe sourcing during this time period.

5.1. Paleoredox Environment of the Proto-North Atlantic: Mo and Biomarker Records

[20] The redox conditions at each site are independently constrained by previous studies [*Brumsack*, 1980; *Kuhnt et al.*, 1997; *Kuypers et al.*, 2002, 2004; *Tsikos et al.*, 2004; *Hetzel et al.*, 2009] and through our use of Mo abundances. Molybdenum provides an effective, independent constraint on the paleoredox conditions of the local settings [*Scott et al.*, 2008; *Scott and Lyons*, 2012]. Specifically, no enrichment (i.e., crustal values of 1 to 2 ppm) is expected under oxic conditions compared to enrichments of 10 to 30 ppm in 'suboxic' settings (defined by low oxygen bottom waters but

[1]Auxiliary materials are available in the HTML. doi:10.1029/2012PA002328.

with H_2S confined to the pore waters) and the roughly 40 to hundreds of ppm levels that characterize euxinia [*Lyons et al.*, 2009]. Molybdenum enrichments are controlled by ambient redox conditions in the water column and sediment, in particular the availability of hydrogen sulfide and organic carbon and the starting concentration of Mo in the basin or ocean [e.g., *Helz et al.*, 1996; *Algeo and Lyons*, 2006; *Lyons et al.*, 2009]. Euxinic enrichments are diagnostically high and variable, principally tracking TOC availability and the dissolved Mo inventory in the local and/or global setting.

[21] Our Mo data (Figure 3) confirm previous findings that euxinic conditions were more pervasive in the southern part of the proto-North Atlantic than in the north [*Trabucho Alexandre et al.*, 2010]. The highest concentrations were observed at site 367 (maximum value of 412 ppm), which is also the site with the highest TOC concentrations and reported occurrences of the molecular fossils isorenieratane and chlorobactane, suggesting that hydrogen sulfide was present in the water column and extended into the photic zone [*Kuypers et al.*, 2002]. Although the maximum TOC concentrations and biomarkers indicative of shallow euxinia are associated with the OAE proper, they initiate before the onset of the OAE as defined by the positive C-isotope excursion (Figure 2) [*Kuypers et al.*, 2002]. Molybdenum enrichments consistent with euxinic conditions are observed at all four southern sites even before the expansion of ocean anoxia that defines the OAE, in contrast to the limited evidence for euxinia in the north. A notable feature of the Demerara Rise (1258) and Tarfaya (S75) sites is a marked *decrease* in Mo concentrations during the OAE, an observation that was also highlighted by *Hetzel et al.* [2009] for other sites along the Demerara Rise shelf transect. The lack of a concurrent decrease in TOC across these intervals suggests that—rather than waning euxinia or a drop in TOC content—these muted Mo enrichments reflect a shift in the Mo inventory, perhaps on a broad scale. If we are correct, this Mo pattern marks a transition from dominantly local to regional/oceanic euxinia and back, with a corresponding depletion in the seawater Mo reservoir during the period of expanded euxinia. Such expansion may have extended across a wide part of the ocean. Site 367 shows concentrations as high as 200 ppm during the OAE, which is still a drop compared to the pre-OAE enrichments. The incomplete core recovery at this site, however, may preclude evidence for the full drop in Mo enrichment we expect during the OAE.

[22] At the northern sites 603B and 105, Mo enrichments are confined to the OAE (Figure 3). Frequent fluctuations in Mo concentrations at these sites during the OAE generally match variations in lithology and TOC contents, suggesting varying redox conditions rather than reservoir effects. At the Eastbourne locale, Mo shows uniformly low values throughout the sampled interval, with concentrations typically below the 1 to 2 ppm crustal average. These data, along with the prevailing Fe relationships (see below), indicate that this site was dominantly if not persistently oxic. In fact, the lowest values for Mo fall below the crustal average and likely reflect average detrital inputs with concentrations reduced by substantial dilution by high carbonate inputs. However, a suite of redox proxies that are particularly sensitive to the early onset of ocean deoxygenation (specifically, Ca-normalized I, Ce, and Mn concentrations) suggest that even the shallow waters at Eastbourne experienced some degree of oxygen depletion before and during the OAE [*Lu et al.*, 2010], although there is no indication that bottom water ever became anoxic or euxinic at this site. We can now view the Fe distributions and likely sources among these sites within a paleoredox context informed by straightforward patterns of Mo enrichment.

5.2. Iron Release From the Oxic Continental Shelf

[23] We begin our discussion of Fe with the most oxic site. The coastal Eastbourne locale shows Fe_T/Al ratios typically at or below the continental crustal average of ca. ~0.5. This average is assumed to represent typical siliciclastic (detrital) input. The Eastbourne samples are complicated by their high carbonate contents (mean ~85%); but Fe_T/Al averages for carbonates are, if anything, typically elevated (~0.9) compared with average continental crust [*Turekian and Wedepohl*, 1961]. In this light, the average Fe_T/Al ratios of 0.46 over the ~20 m are consistent with net loss of Fe from the sediments. Loss of Fe, which should be isotopically light [*Severmann et al.*, 2010], is further indicated by the observation that the $\delta^{56}Fe_T$ data cluster slightly above 0‰ with an average of +0.08‰ (Figures 3 and 4). Sedimentary Fe reduction promoted Fe build up in the pore fluids and, with pervasive bioturbation, transport from the sediment [*Lyons and Severmann*, 2006; *Severmann et al.*, 2010]. These conditions were ultimately facilitated by a lack of appreciable sulfate reduction due to the overall paucity of organic matter at this site (average TOC contents are 0.12 wt. %). The results at Eastbourne for Fe_T/Al and $\delta^{56}Fe_T$ are invariant before, during, and after the OAE, defined by the $\delta^{13}C$ excursion (Figure 2). The lowest $\delta^{56}Fe_T$ value is from a sample that also shows slightly higher Fe_T/Al ratios and could reflect transient euxinia, consistent with the evidence for low oxygen from *Lu et al.* [2010]. Nevertheless, the Eastbourne data generally point to dominantly oxic deposition, with robust signals that are not complicated by the very high carbonate contents.

5.3. Iron Cycling in the Southern Basin: Hydrothermal Sources and Euxinic Sinks

[24] Our highest Fe_T/Al ratios, with several samples exceeding values of 2, were measured during the OAE at the southern site 367 and site 105 in the north (Figures 3 and 4). Surface sediments representing the current euxinic stage in the Black Sea, our best modern analog, have markedly elevated Fe_T/Al ratios when compared to average continental crust. The magnitude of the enrichment as driven by the Fe shuttle is constrained by sedimentation rates and the mass balance of the source-to-sink relationship [*Raiswell and Anderson*, 2005; *Lyons and Severmann*, 2006]. Nevertheless, Fe_T/Al values exceeding 1.2, as we have observed during OAE-2, are higher than those recorded in the modern unit 1 of the Black Sea and are only rarely observed throughout the Phanerozoic. As such, more extreme Fe enrichments, exceeding ~1.5, may be a flag signaling hydrothermal augmentation [*Cruse and Lyons*, 2004] or secondary remobilization within the sediment column. Broader tectonic and paleogeographic parameters must also be considered.

[25] Due to its location on the ancestral mid-ocean ridge, DSDP site 144 is the best candidate among our study sites

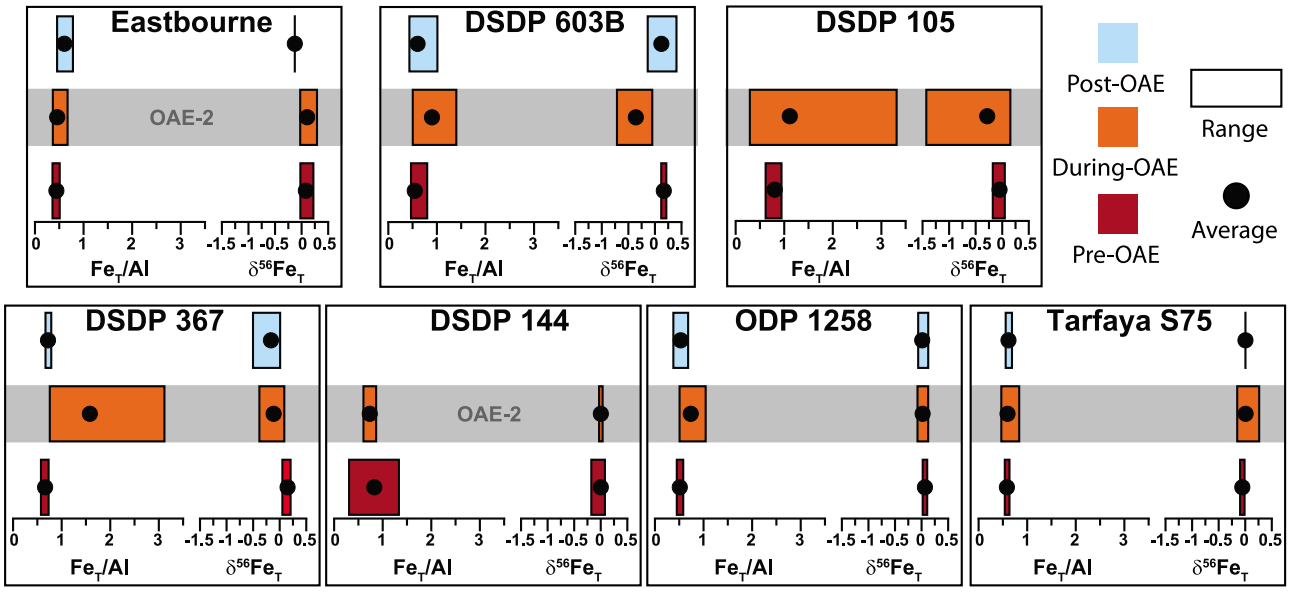

Figure 4. Averages and ranges for the iron isotope data and Fe concentrations (relative to Al) at each section before, during, and after OAE-2.

for a strong hydrothermal signal from ridge-style venting. This locale shows high Fe_T/Al ratios before the OAE (average 0.83), with smaller enrichments during the OAE (0.73) and marked variability in the magnitude of enrichment. All the Fe isotope data are relatively uniform, including the data corresponding with the Fe enrichments, with pre-OAE and syn-OAE $\delta^{56}Fe_T$ averages of 0.00‰. Because hydrothermal Fe and background detrital sources of Fe have similar isotopic properties, pronounced Fe enrichment (high Fe_T/Al) without parallel isotopic variability should be diagnostic of hydrothermal inputs. The pervasive euxinic conditions throughout the southern part of the proto-North Atlantic and associated low Fe solubility under sulfidic conditions, in combination with the pattern of oceanic circulation, likely aided in the relatively short dispersal distance of hydrothermal Fe to the nearby southern sites with little associated isotope fractionation during transport.

[26] The shelfal Fe shuttle likely contributed Fe to at least one of our southern sites, specifically the deepest site 367, which has some of the most negative $\delta^{56}Fe_T$ values among the four southern sites (minimum $\delta^{56}Fe_T = -0.50‰$). That said, the lack of a continuous negative shift in $\delta^{56}Fe_T$ that tracks the level of Fe enrichment argues for a shuttle signal that, if present, was typically swamped by hydrothermal Fe with a $\delta^{56}Fe_T$ near 0‰. The data at site 1258 (Figure 4) do not argue for significant source variations based on the Fe isotope records before, during, and after the OAE (with averages of 0.09, 0.04, 0.07‰, respectively) despite Fe_T/Al ratios that increase significantly during the event (average pre-OAE: 0.50, during: 0.70, and post-OAE: 0.47). *Clayton et al.* [2007] analyzed Fe isotopes at another Demerara Rise site, ODP 1260, with low sample resolution that does not cover the OAE and methods that focused on separate Fe minerals. It is difficult therefore to compare their data to ours. The most reasonable interpretation is that the Fe delivered to this site is dominantly from a hydrothermal source, although a subtle negative shift at the end of the OAE may reflect input via the shuttle. The pronounced Mo enrichments suggest persistently euxinic deposition at this site before, during, and after the OAE. Comparatively low Fe enrichments before and after OAE-2 likely mirror the inefficiency by which hydrothermal and/or shuttled Fe is transported to a locally euxinic site via the surrounding oxic ocean. In contrast, suppressed signals during the event reflect the 'competition' for hydrothermal and shuttled Fe under the spatially extensive sulfidic conditions in the southern portion of the proto-North Atlantic.

[27] At the shallow Tarfaya shelf site S75, high sedimentation rates may have favored dilution of the hydrothermal signal by detritally sourced Fe, consistent with relatively smaller Fe enrichments compared to the other southern sites (Figures 3 and 4). Despite its location on the continental shelf—and in contrast to our northern shelf site from Eastbourne—there is no indication that site S75 acted as an iron source at any time around OAE-2. These Fe isotope data agree well with those generated for a different Tarfaya shelf section, S57, by *Jenkyns et al.* [2007]. They too show relatively small isotopic variability with values near 0‰. In general, the details of the Fe mass balance, the transport mechanisms, and the local/regional overprints, including spatially varying hydrothermal inputs, remain incompletely defined pending additional analyses at other sites and more general exploration of the mechanisms behind benthic Fe fluxes and basin-ward transport. Nevertheless, the relatively stable $\delta^{56}Fe_T$ throughout the measured section (overall average of 0.00‰) and only slightly elevated but consistent Fe_T/Al (overall average of 0.60), our data are best explained by high terrigenous inputs against a relatively small source of hydrothermal Fe, which mildly enriched the Fe without shifting the isotopic composition appreciably.

[28] Despite our claim above for possible inputs via the Fe shuttle, the narrow range in $\delta^{56}Fe_T$ between −0.5 and 0.0‰ at site 367, despite a large range in Fe_T/Al (0.57 to 3.12), is most consistent with a signal dominated by hydrothermal sources for the excess reactive Fe observed during OAE-2. The same hydrothermal dominance likely applies for the

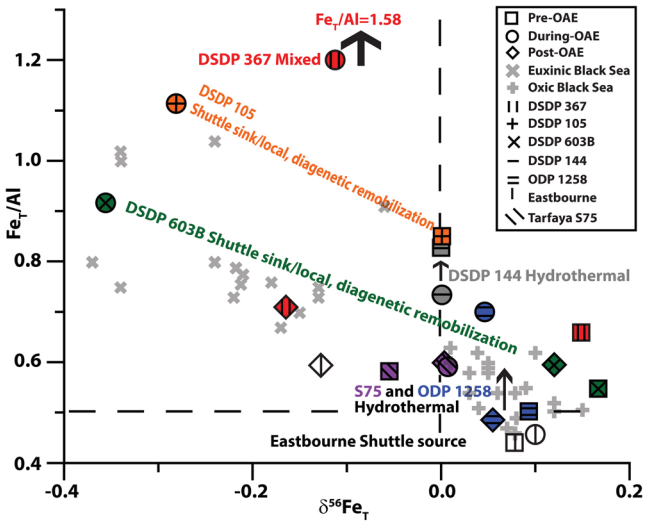

Figure 5. The $\delta^{56}Fe_T$ averages for each site grouped as pre (open square), post (open diamond) and during (open circle) OAE-2. In the background are data from euxinic (gray "x") and oxic (gray "plus") [*Severmann et al.*, 2008]. Post-OAE $\delta^{56}Fe_T$ at Eastbourne is represented by only one data point. Black dashed lines indicate average crustal values. Note that DSDP 144 is proximal to a mid-ocean ridge, and S75 and ODP 1258 are distal. Generally, sites 144, S75 and 1258 show variable Fe_T/Al enrichment without sympathetic isotopic change suggesting hydrothermal sourcing, but with different magnitudes of enrichment as a function of position relative to ridge.

other southern sites (DSDP 144, ODP 1258, and Tarfaya S75). All four sites show moderate (in the case of S75) to intense (site 367) enrichments in reactive Fe (Figures 3 and 4), poor correlation between Fe_T/Al and $\delta^{56}Fe_T$ (Figure 5) and Fe isotope compositions near 0‰. These relationships are even expressed by the samples with highly elevated Fe_T/Al ratios. The source of the Fe might be linked to faster spreading rates and attendant increased hydrothermal venting within the basin [*Conrad and Lithgow-Bertelloni*, 2007] or emplacement of the Caribbean LIP in the equatorial Eastern Pacific [*Sinton and Duncan*, 1997], which may have triggered OAE-2, although long-distance Fe transport is challenged by the low solubility of Fe in euxinic and, in particular, oxic waters. While sites 1258 and S75 show relatively small ranges in Fe_T/Al ratios (averaging 0.54 and 0.60, respectively) and isotope compositions (averaging 0.06 and 0.00‰, respectively) throughout the entire sections, site 367 shows marked Fe_T/Al enrichment during the OAE (average 1.58) with a relatively small negative $\delta^{56}Fe_T$ shift (average −0.11‰), perhaps, pointing to locally sourced Fe tied to mid-ocean ridge venting.

5.4. Iron Cycling in the Northern Basin: Diagenetic Overprinting and the Shuttle

[29] In contrast to the southern sites, the two northern localities, DSDP 603B and DSDP 105, do not show Mo enrichments before the OAE, implying that conditions remained largely oxic. However, despite the lack of Mo enrichments, site 105 shows elevated Fe_T/Al ratios that coincide with intermittent periods of black shale deposition even before the OAE (see lithostratigraphy in Figure 2), which could mark anoxic conditions that were only weakly sulfidic. The OAE yielded samples at both sites with significantly elevated Fe_T/Al ratios, and black shales became more abundant, although oxic conditions likely dominated based on the lithostratigraphy and only slightly elevated Mo contents. Furthermore, both sites show high-low oscillations in Fe_T/Al roughly similar to the variability observed in TOC contents and lithofacies patterns (Figures 2 and 3). Although the northern site 105 and southern site 367 have similarly large Fe enrichments, we infer based on its large negative shifts in $\delta^{56}Fe_T$ that site 105 received very little, perhaps, no hydrothermally sourced Fe.

[30] The distinctly negative Fe isotope values (min. $\delta^{56}Fe_T = -1.43$‰) measured at site 105 are similar to values measured by *Jenkyns et al.* [2007] in the Scaglia Bianca at Furlo, Italy (min. $\delta^{56}Fe_T = -1.7$‰), and the sites share similar lithostratigraphic patterns—with relatively thin black shale units intercalated within dominantly bioturbated oxic units. In the case of the Scaglia Bianca, shale units alternate with cherty limestones; at site 105 the laminated shales alternate with green claystones. The pattern of seemingly rapid $\delta^{56}Fe_T$ variability could suggest redox controls during the OAE that correlate with the varying sedimentary facies, with positive $\delta^{56}Fe_T$ for the bioturbated sediments and negative $\delta^{56}Fe_T$ for the laminated organic-rich black shales. Such a relationship could reflect time-varying operation of the shuttle model over short, perhaps orbital, time scales. More likely, however, is small-scale diagenetic remobilization of Fe within the sediment column, yielding Fe-poor to Fe-rich layers. Although the depositional conditions may have been dominantly oxic, some elevated molybdenum concentrations (in all lithologies) at sites 105 and 603B are consistent with transiently euxinic episodes during the OAE at these sites as also recorded in the organic richness of the black shales. However, the predominance of comparatively low Mo concentrations (OAE averages at sites 105 and 603 of 16 and 18 ppm, respectively) argues against persistent euxinia [see *Scott and Lyons*, 2012] and suggests that the observed Fe patterns could be a secondary phenomenon tied mostly to stratigraphic variability in TOC content. Specifically, we argue that the data reflect Fe mobilization within the sediments, whereby the organic- and sulfide-rich black shales capture Fe that is released from adjacent layers lacking organic matter and thus favoring bacterial iron reduction over sulfate reduction. Similar processes can be observed today in the Black Sea where a sulfidization front is formed by the opposing gradient between an organic-rich marine sapropel and an organic-lean but Fe-rich limnic unit [*Neretin et al.*, 2004]. Our Fe paleoredox proxies must thus be used with caution when interpreting juxtapositions (interlayering) of sediments with very different concentrations of TOC—or methane, in the case of sulfate reduction driven by AOM (anaerobic oxidation of methane). In a sense, though, the post-depositional remobilization and repartitioning of Fe mirrors the processes of the Fe shuttle, which, by contrast, operates on a basin scale rather than within the sediment column. In other words, isotopically light Fe migrates from organic-poor layers dominated by reductive Fe mobilization to organic- and sulfide-rich layers where the remobilized iron is recaptured quantitatively as pyrite. These two facies

reflect dominantly oxic deposition and at least transient euxinia, respectively.

[31] Of all the sites investigated, site 603B shows the most convincing fingerprint of enrichment via the Fe shuttle, with nearly all of the samples (11 out of 14) demonstrating a systematic anti-correlation between $\delta^{56}Fe_T$ and Fe_T/Al (Figure 5) that is similar to the trend defined by Black Sea sediments. During the OAE, site 603B shows overall enrichments in Fe_T/Al (average: 0.92) and more negative $\delta^{56}Fe_T$ values (average: −0.36‰)—compared to pre- and post-OAE Fe_T/Al values that fall close to crustal averages (0.56 and 0.61, respectively), with $\delta^{56}Fe_T$ values that are shifted heavy compared to average crust (pre-OAE average: 0.17‰; post-OAE average: 0.12‰). Importantly, the high average Fe concentration and negative average $\delta^{56}Fe_T$ during the OAE were calculated using all the data, regardless of the lithofacies, and the largest Mo concentrations (extending up to 64 ppm) generally correlate with the more negative $\delta^{56}Fe_T$. Unlike site 105, the Fe and Mo data point to a high frequency and persistence of euxinia during the OAE at site 603B, making it a better candidate for Fe inputs via the iron shuttle, despite lithologic observations from site 603B that indicate marked redox-transitions similar to those of site 105. Of course, diagenetic remobilization could overprint the primary shuttle signals. Most obvious is the challenge we face in untangling the shuttle signal from possible diagenetic overprint in sediments marked by alternating and thinly bedded organic-rich and organic-lean intervals.

5.5. Synthesis

[32] Figures 4 and 5 provide us with a way to simplify a complex data set. For example, although there are similarities in their Fe_T/Al ratios, we note a distinctly smaller range in $\delta^{56}Fe_T$ values at site 367 compared to those at site 105 (Figure 4), which likely points to differences in the Fe sources and enrichment processes. Past work has revealed a straightforward relationship between Fe_T/Al ratios and $\delta^{56}Fe_T$ seen at diverse times and places in the geologic record [e.g., *Johnson et al.*, 2008]. In the absence of strong hydrothermal inputs, euxinic enrichments in reactive iron expressed as elevated Fe_T/Al ratios have consistently resulted in lower $\delta^{56}Fe_T$ values, mirroring corresponding Fe loss at shallow, oxic source regions—i.e., our shuttle model. These benthic processes at oxic sites leave a fingerprint of lowered Fe_T/Al with correspondingly heavy $\delta^{56}Fe_T$. Along these lines, a systematic trend is observed between Fe_T/Al ratios and $\delta^{56}Fe_T$ in the modern, Black Sea [*Severmann et al.*, 2008] and in ancient epicontinental Devonian shales [*Duan et al.*, 2010]. We assert that such processes likely operated during OAE-2 (Figure 5), although the signals are far more complex because of the much larger spatial scale of Fe cycling in the Cretaceous proto-Atlantic Ocean and the likelihood of large and pervasive hydrothermal inputs associated with activity along mid-ocean ridges within that basin.

6. Conclusions

[33] The Fe cycle in the proto-North Atlantic during the Cretaceous is, not surprisingly, complex with multiple sources and sinks whose relative roles vary with position in the basin. The highly productive and anoxic shelves of the southern equatorial portions served as sinks, while the oxic shelves of the northern proto-North Atlantic seem to have served as Fe sources. Our data show that the southern portion of the proto-North Atlantic was influenced by hydrothermal Fe, but with a large portion of the northern basin lacking evidence for significant hydrothermal inputs. This contrast might reflect the difficulty of transporting Fe a significant distance in an oxic or sulfidic water column, since iron oxides and pyrite quickly precipitate and settle. Although Fe is more soluble in a sulfidic water column relative to oxic waters, pyrite precipitation poses a challenge to transporting Fe the great distances needed to enrich all of the proto-North Atlantic, whether sourced by hydrothermal or shuttle inputs. Our most enriched sites are restricted to the southern proto-North Atlantic and, based on the combined Fe_T/Al and $\delta^{56}Fe_T$ data, argue for an iron cycle dominated by hydrothermal inputs, although site 367 likely bears the low-temperature impact of the shuttle as well.

[34] When the data from this study are plotted with those from the Black Sea (Figure 5), the northern sites (Eastbourne, 603B, and 105) are consistent with the predictions for shuttled Fe—i.e., Fe enrichments or depletions that vary systematically and antithetically with the Fe isotope trend. On the other hand, the Fe trends at 105 and 603B could reasonably be tied to secondary remobilization during burial diagenesis. We argue, particularly for site 603B, that both of these mechanisms are recorded. The potential for diagenetic overprints offers a cautionary note, but it is our good fortune that such overprints can be independently anticipated by the often fine stratigraphic scale of extreme geochemical variability they reflect (e.g., sapropel layers in an package of otherwise oxic sediments). We can expect oxically deposited, organic-lean beds marked by Fe loss and a residual, heavy isotopic signature in close proximity to organic-rich shales with correspondingly high Fe concentrations and low isotopic compositions. Also, we can predict fundamentally different sulfur isotope properties for pyrite formed via the two scenarios (shuttle versus diagenetic remobilization), with primary, water column-formed euxinic pyrite often showing very light and uniform $\delta^{34}S$ values [*Lyons*, 1997; *Lyons et al.*, 2003] compared to secondary, diagenetic pyrite tied to Fe remobilization, which can be marked by pronounced $\delta^{34}S$ enrichments [*Jørgensen et al.*, 2004]. The organic biomarkers for photic euxinia also provide independent insight. The hydrothermal signals, by contrast, should enrich Fe_T/Al without appreciable parallel variability in the $\delta^{56}Fe_T$.

[35] Many authors have postulated that a major hydrothermal pulse predated the OAE and may have catalyzed the large positive carbon isotope excursion of the anoxic event through expanded primary production—perhaps linked to increased inputs of Fe and its importance as a micronutrient [*Jenkyns*, 2010, and references therein]. Our data support the presence of hydrothermal inputs, particularly in the southern proto-North Atlantic, and it is probably not a coincidence that this is the same portion of the basin that shows the strongest evidence for persistent and pervasive euxinia [see also *Jenkyns*, 2010]. Nevertheless, the hydrothermal signal is neither consistently strong nor basin-wide; its global role as an essential OAE precursor awaits additional study.

[36] Although complex, the Fe signals demonstrate that there were multiple Fe sources operating in the proto-North Atlantic before, during, and after the OAE. Unlike most past

applications of the Fe proxies, our study captures processes operating on the scale of an ocean basin with an active mid-ocean ridge, in contrast to the marginal basins and epicontinental seas that have been emphasized in many past studies of Fe paleoproxies. Not surprisingly, the signals are confounded by the challenges of transporting Fe long distances under both oxic and anoxic-sulfidic conditions, given its insolubility in both cases. Furthermore, the vast spatial extents of Fe sequestration under large-scale euxinia place high demands on the end-member sources and specifically their abilities to dominate the Fe archived in the sediments at any particular site. We should expect that the elemental and isotopic signals are subtle in a system of this size, and they are. Our most important take-home message may be that the proto-Atlantic received elevated Fe inputs from several sources and that the redox state of the basin was not exclusively euxinic during OAE-2. Both results point to previously unknown heterogeneity in depositional conditions and the associated biogeochemical cycling of iron.

[37] **Acknowledgments.** Financial support was provided by the NSF. We would like to thank Steve Bates, Bill Gilhooly, Ben Gill, Gordon Love, Mike McKibben, Noah Planavsky, Robert Raiswell, Chris Reinhard, and Clint Scott for helpful discussions in the early stages of this manuscript. We would also like to thank Walter Hale for access to IODP samples at the Bremen Core Repository, Germany. We thank Hugh Jenkyns and one anonymous reviewer, as well as the Editor, Rainer Zahn, for constructive comments that have helped to improve the manuscript.

References

Adams, D. D., M. T. Hurtgen, and B. B. Sageman (2010), Volcanic triggering of a biogeochemical cascade during Oceanic Anoxic Event 2, *Nat. Geosci.*, *3*(3), 201–204, doi:10.1038/ngeo743.

Algeo, T. J., and T. W. Lyons (2006), Mo–total organic carbon covariation in modern anoxic marine environments: Implications for analysis of paleoredox and paleohydrographic conditions, *Paleoceanography*, *21*, PA1016, doi:10.1029/2004PA001112.

Anderson, T. F., and R. Raiswell (2004), Sources and mechanisms for the enrichment of highly reactive iron in euxinic Black Sea sediments, *Am. J. Sci.*, *304*(3), 203–233, doi:10.2475/ajs.304.3.203.

Arnold, G. L., S. Weyer, and A. D. Anbar (2004), Fe Isotope Variations in Natural Materials Measured Using High Mass Resolution Multiple Collector ICPMS, *Anal. Chem.*, *76*(2), 322–327, doi:10.1021/ac034601v.

Arthur, M. A., W. E. Dean, and L. M. Pratt (1988), Geochemical and climatic effects of increased marine organic carbon burial at the Cenomanian/Turonian boundary, *Nature*, *335*(6192), 714–717, doi:10.1038/335714a0.

Barron, E. J. (1983), A warm, equable Cretaceous: The nature of the problem, *Earth Sci. Rev.*, *19*(4), 305–338, doi:10.1016/0012-8252(83)90001-6.

Beard, B. L., C. M. Johnson, J. L. Skulan, K. H. Nealson, L. Cox, and H. Sun (2003), Application of Fe isotopes to tracing the geochemical and biological cycling of Fe, *Chem. Geol.*, *195*(1–4), 87–117, doi:10.1016/S0009-2541(02)00390-X.

Bennett, S. A., O. Rouxel, K. Schmidt, D. Garbe-Schönberg, P. J. Statham, and C. R. German (2009), Iron isotope fractionation in a buoyant hydrothermal plume, 5°S Mid-Atlantic Ridge, *Geochim. Cosmochim. Acta*, *73*(19), 5619–5634, doi:10.1016/j.gca.2009.06.027.

Berger, W. H., and U. von Rad (1972), Cretaceous and Cenozoic sediments from the Atlantic Ocean, *Initial Rep. Deep Sea Drill. Proj.*, *14*, 787–886, doi:10.2973/dsdp.proc.14.126.1972.

Blain, S., S. Bonnet, and C. Guieu (2008), Dissolved iron distribution in the tropical and sub tropical South Eastern Pacific, *Biogeosciences*, *5*, 269–280, doi:10.5194/bg-5-269-2008.

Blättler, C. L., H. C. Jenkyns, L. M. Reynard, and G. M. Henderson (2011), Significant increases in global weathering during Oceanic Anoxic Events 1a and 2 indicated by calcium isotopes, *Earth Planet. Sci. Lett.*, *309*(1–2), 77–88, doi:10.1016/j.epsl.2011.06.029.

Bruland, K. W., E. L. Rue, G. J. Smith, and G. R. DiTullio (2005), Iron, macronutrients and diatom blooms in the Peru upwelling regime: Brown and blue waters of Peru, *Mar. Chem.*, *93*(2–4), 81–103, doi:10.1016/j.marchem.2004.06.011.

Brumsack, H. J. (1980), Geochemistry of Cretaceous black shales from the Atlantic Pcean (DSDP Legs 11, 14, 36 and 41), *Chem. Geol.*, *31*(0), 1–25, doi:10.1016/0009-2541(80)90064-9.

Canfield, D. E., T. W. Lyons, and R. Raiswell (1996), A model for iron deposition to euxinic Black Sea sediments, *Am. J. Sci.*, *296*(7), 818–834, doi:10.2475/ajs.296.7.818.

Clayton, R. E., A. J. Nederbragt, D. Malinovsky, P. Andersson, and J. Thurow (2007), Data report: Iron isotope geochemistry of mid-Cretaceous organic-rich sediments at Demerara Rise (ODP Leg 207), *Proc. Ocean Drill Program Sci. Results*, *207*, 14 pp., doi:10.2973/odp.proc.sr.207.109.2006.

Conrad, C. P., and C. Lithgow-Bertelloni (2007), Faster seafloor spreading and lithosphere production during the mid-Cenozoic, *Geology*, *35*(1), 29–32, doi:10.1130/G22759A.1.

Coplen, T. B. (2011), Guidelines and recommended terms for expression of stable-isotope-ratio and gas-ratio measurement results, *Rapid Commun. Mass Spectrom.*, *25*(17), 2538–2560.

Cruse, A. M., and T. W. Lyons (2004), Trace metal records of regional paleoenvironmental variability in Pennsylvanian (Upper Carboniferous) black shales, *Chem. Geol.*, *206*(3–4), 319–345, doi:10.1016/j.chemgeo.2003.12.010.

Czaja, A. D., C. M. Johnson, B. L. Beard, J. L. Eigenbrode, K. H. Freeman, and K. E. Yamaguchi (2010), Iron and carbon isotope evidence for ecosystem and environmental diversity in the ∼2.7 to 2.5 Ga Hamersley Province, Western Australia, *Earth Planet. Sci. Lett.*, *292*(1–2), 170–180, doi:10.1016/j.epsl.2010.01.032.

Duan, Y., S. Severmann, A. D. Anbar, T. W. Lyons, G. W. Gordon, and B. B. Sageman (2010), Isotopic evidence for Fe cycling and repartitioning in ancient oxygen-deficient settings: Examples from black shales of the mid-to-late Devonian Appalachian basin, *Earth Planet. Sci. Lett.*, *290*(3–4), 244–253, doi:10.1016/j.epsl.2009.11.052.

Elrod, V., W. Berelson, K. Coale, and K. Johnson (2004), The flux of iron from continental shelf sediments: A missing source for global budgets, *Geophys. Res. Lett.*, *31*, L12307, doi:10.1029/2004GL020216.

Erbacher, J., O. Friedrich, P. A. Wilson, H. Birch, and J. Mutterlose (2005), Stable organic carbon isotope stratigraphy across Oceanic Anoxic Event 2 of Demerara Rise, western tropical Atlantic, *Geochem. Geophys. Geosyst.*, *6*, Q06010, doi:10.1029/2004GC000850.

Frijia, G., and M. Parente (2008), Strontium isotope stratigraphy in the upper Cenomanian shallow-water carbonates of the southern Apennines: Short-term perturbations of marine 87Sr/86Sr during the oceanic anoxic event 2, *Palaeogeogr. Palaeoclimatol. Palaeoecol.*, *261*(1–2), 15–29, doi:10.1016/j.palaeo.2008.01.003.

Gale, A. S. (1996), Turonian correlation and sequence stratigraphy of the Chalk in southern England, in *Sequence Stratigraphy in British Geology*, edited by S. E. Hesselbo and D. N. Parkinson, *Geol. Soc. Spec. Publ.*, *103*, 177–195, doi:10.1144/GSL.SP.1996.103.01.10.

Halverson, G. P., F. Poitrasson, P. F. Hoffman, A. Nédélec, J.-M. Montel, and J. Kirby (2011), Fe isotope and trace element geochemistry of the Neoproterozoic syn-glacial Rapitan iron formation, *Earth Planet. Sci. Lett.*, *309*(1–2), 100–112, doi:10.1016/j.epsl.2011.06.021.

Hayes, D. E., A. C. Pimm, W. E. Benson, W. H. Berger, U. von Rad, P. R. Supko, J. P. Beckmann, and P. H. Roth (1972), Sites 143 and 144, *Initial Rep. Deep Sea Drill. Proj.*, *14*, 283–301.

Helz, G. R., C. V. Miller, J. M. Charnock, J. F. W. Mosselmans, R. A. D. Pattrick, C. D. Garner, and D. J. Vaughan (1996), Mechanism of molybdenum removal from the sea and its concentration in black shales: EXAFS evidence, *Geochim. Cosmochim. Acta*, *60*(19), 3631–3642, doi:10.1016/0016-7037(96)00195-0.

Herbin, J. P., L. Montadert, C. Muller, R. Gomez, J. Thurow, and J. Wiedmann (1986), Organic-rich sedimentation at the Cenomanian-Turonian boundary in oceanic and coastal basins in the North Atlantic and Tethys, in *North Atlantic Palaeoceanography*, edited by C. P. Summerhayes and N. J. Shackleton, *Geol. Soc. Spec. Publ.*, *21*, 389–422, doi:10.1144/GSL.SP.1986.021.01.28.

Herbin, J. P., E. Masure, and J. Roucaché (1987), Cretaceous formations from the lower continental rise off Cape Hatteras: Organic geochemistry, dinoflagelate cysts, and the Cenomanian/Turonian boundary event at Sites 603(Leg 93) and 105(Leg 11), *Initial Rep. Deep Sea Drill. Proj.*, *93*, 1139–1160, doi:10.2973/dsdp.proc.93.147.1987.

Hetzel, A., M. E. Böttcher, U. G. Wortmann, and H.-J. Brumsack (2009), Paleo-redox conditions during OAE 2 reflected in Demerara Rise sediment geochemistry (ODP Leg 207), *Palaeogeogr. Palaeoclimatol. Palaeoecol.*, *273*(3–4), 302–328, doi:10.1016/j.palaeo.2008.11.005.

Hollister, C. D., J. I. Ewing, D. Habib, J. C. Hathaway, Y. Lancelot, H. Luterbacher, F. J. Paulus, F. J. Poag, J. A. Wilcoxon, and P. Worstell (1972), Site 105: Lower continental rise hills, *Initial Rep. Deep Sea Drill. Proj.*, *11*, 219–312, doi:10.2973/dsdp.proc.11.106.1972.

Huber, B. T., D. A. Hodell, and C. P. Hamilton (1995), Middle-Late Cretaceous climate of the southern high latitudes: Stable isotopic evidence for minimal equator-to-pole thermal gradients, *Geol. Soc. Am. Bull.*, *107*(10), 1164–1191, doi:10.1130/0016-7606(1995)107<1164:MLCCOT>2.3.CO;2.

Jenkyns, H. C. (2010), Geochemistry of oceanic anoxic events, *Geochem. Geophys. Geosyst.*, *11*, Q03004, doi:10.1029/2009GC002788.

Jenkyns, H. C., A. Matthews, H. Tsikos, and Y. Erel (2007), Nitrate reduction, sulfate reduction, and sedimentary iron isotope evolution during the Cenomanian-Turonian oceanic anoxic event, *Paleoceanography*, *22*, PA3208, doi:10.1029/2006PA001355.

Jiménez Berrocoso, Á., K. G. MacLeod, S. E. Calvert, and J. Elorza (2008), Bottom water anoxia, inoceramid colonization, and benthopelagic coupling during black shale deposition on Demerara Rise (Late Cretaceous western tropical North Atlantic), *Paleoceanography*, *23*, PA3212, doi:10.1029/2007PA001545.

Johnson, C. M., B. L. Beard, and E. E. Roden (2008), The iron isotope fingerprints of redox and biogeochemical cycling in modern and ancient Earth, *Annu. Rev. Earth Planet. Sci.*, *36*(1), 457–493, doi:10.1146/annurev.earth.36.031207.124139.

Jones, C. E., and H. C. Jenkyns (2001), Seawater strontium isotopes, oceanic anoxic events, and seafloor hydrothermal activity in the Jurassic and Cretaceous, *Am. J. Sci.*, *301*(2), 112–149, doi:10.2475/ajs.301.2.112.

Jørgensen, B. B., M. E. Böttcher, H. Lüschen, L. N. Neretin, and I. I. Volkov (2004), Anaerobic methane oxidation and a deep H_2S sink generate isotopically heavy sulfides in Black Sea sediments, *Geochim. Cosmochim. Acta*, *68*(9), 2095–2118, doi:10.1016/j.gca.2003.07.017.

Keller, G., Q. Han, T. Adatte, and S. J. Burns (2001), Palaeoenvironment of the Cenomanian-Turonian transition at Eastbourne, England, *Cretaceous Res.*, *22*(4), 391–422, doi:10.1006/cres.2001.0264.

Kolonic, S., et al. (2005), Black shale deposition on the northwest African Shelf during the Cenomanian/Turonian oceanic anoxic event: Climate coupling and global organic carbon burial, *Paleoceanography*, *20*, PA1006, doi:10.1029/2003PA000950.

Kuhnt, W., A. Nederbragt, and L. Leine (1997), Cyclicity of Cenomanian-Turonian organic-carbon-rich sediments in the Tarfaya Atlantic Coastal Basin (Morocco), *Cretaceous Res.*, *18*(4), 587–601, doi:10.1006/cres.1997.0076.

Kuhnt, W., F. Luderer, S. Nederbragt, J. Thurow, and T. Wagner (2005), Orbital-scale record of the late Cenomanian-Turonian oceanic anoxic event (OAE-2) in the Tarfaya Basin (Morocco), *Int. J. Earth Sci.*, *94*(1), 147–159, doi:10.1007/s00531-004-0440-5.

Kuroda, J. (2007), Contemporaneous massive subaerial volcanism and late cretaceous Oceanic Anoxic Event 2, *Earth Planet. Sci. Lett.*, *256*(1–2), 211–223, doi:10.1016/j.epsl.2007.01.027.

Kuypers, M. M. M., R. D. Pancost, I. A. Nijenhuis, and J. S. Sinninghe Damsté (2002), Enhanced productivity led to increased organic carbon burial in the euxinic North Atlantic basin during the late Cenomanian oceanic anoxic event, *Paleoceanography*, *17*(4), 1051, doi:10.1029/2000PA000569.

Kuypers, M. M. M., L. J. Lourens, W. I. C. Rijpstra, R. D. Pancost, I. A. Nijenhuis, and J. S. Sinninghe Damsté (2004), Orbital forcing of organic carbon burial in the proto-North Atlantic during oceanic anoxic event 2, *Earth Planet. Sci. Lett.*, *228*(3–4), 465–482, doi:10.1016/j.epsl.2004.09.037.

Leckie, R. M., T. J. Bralower, and R. Cashman (2002), Oceanic anoxic events and plankton evolution: Biotic response to tectonic forcing during the mid-Cretaceous, *Paleoceanography*, *17*(3), 1041, doi:10.1029/2001PA000623.

Lu, Z., H. C. Jenkyns, and R. E. M. Rickaby (2010), Iodine to calcium ratios in marine carbonate as a paleo-redox proxy during oceanic anoxic events, *Geology*, *38*(12), 1107–1110, doi:10.1130/G31145.1.

Lyons, T. W. (1997), Sulfur isotopic trends and pathways of iron sulfide formation in upper Holocene sediments of the anoxic Black Sea, *Geochim. Cosmochim. Acta*, *61*(16), 3367–3382, doi:10.1016/S0016-7037(97)00174-9.

Lyons, T. W., and S. Severmann (2006), A critical look at iron paleoredox proxies: New insights from modern euxinic marine basins, *Geochim. Cosmochim. Acta*, *70*(23), 5698–5722, doi:10.1016/j.gca.2006.08.021.

Lyons, T. W., J. P. Werne, D. J. Hollander, and R. W. Murray (2003), Contrasting sulfur geochemistry and Fe/Al and Mo/Al ratios across the last oxic-to-anoxic transition in the Cariaco Basin, Venezuela, *Chem. Geol.*, *195*, 131–157, doi:10.1016/S0009-2541(02)00392-3.

Lyons, T. W., A. D. Anbar, S. Severmann, C. Scott, and B. C. Gill (2009), Tracking euxinia in the ancient ocean: A multiproxy perspective and proterozoic case study, *Annu. Rev. Earth Planet. Sci.*, *37*(1), 507–534, doi:10.1146/annurev.earth.36.031207.124233.

MacLeod, K. G., E. E. Martin, and S. W. Blair (2008), Nd isotopic excursion across Cretaceous ocean anoxic event 2(Cenomanian-Turonian) in the tropical North Atlantic, *Geology*, *36*(10), 811–814, doi:10.1130/G24999A.1.

Martin, J. H., and S. E. Fitzwater (1988), Iron deficiency limits phytoplankton growth in the north-east Pacific subarctic, *Nature*, *331*(6154), 341–343, doi:10.1038/331341a0.

Moffett, J. W., T. J. Goepfert, and S. W. A. Naqvi (2007), Reduced iron associated with secondary nitrite maxima in the Arabian Sea, *Deep Sea Res., Part I*, *54*(8), 1341–1349, doi:10.1016/j.dsr.2007.04.004.

Neretin, L. N., M. E. Böttcher, B. B. Jørgensen, I. I. Volkov, H. Lüschen, and K. Hilgenfeldt (2004), Pyritization processes and greigite formation in the advancing sulfidization front in the upper Pleistocene sediments of the Black Sea, *Geochim. Cosmochim. Acta*, *68*(9), 2081–2093, doi:10.1016/S0016-7037(03)00450-2.

Pancost, R. D., N. Crawford, S. Magness, A. Turner, H. C. Jenkyns, and J. R. Maxwell (2004), Further evidence for the development of photic-zone euxinic conditions during Mesozoic oceanic anoxic events, *J. Geol. Soc.*, *161*(3), 353–364, doi:10.1144/0016764903-059.

Paul, C. R. C., M. A. Lamolda, S. F. Mitchell, M. R. Vaziri, A. Gorostidi, and J. D. Marshall (1999), The Cenomanian-Turonian boundary at Eastbourne (Sussex, UK): A proposed European reference section, *Palaeogeogr. Palaeoclimatol. Palaeoecol.*, *150*(1–2), 83–121, doi:10.1016/S0031-0182(99)00009-7.

Poulton, S. W., and D. E. Canfield (2005), Development of a sequential extraction procedure for iron: Implications for iron partitioning in continentally derived particulates, *Chem. Geol.*, *214*(3–4), 209–221, doi:10.1016/j.chemgeo.2004.09.003.

Raiswell, R., and T. Anderson (2005), Reactive iron enrichment in sediments deposited beneath euxinic bottom waters: Constraints on supply by shelf recycling, in *Mineral Deposits and Earth Evolution*, edited by I. McDonald et al., *Geol. Soc. Spec. Publ.*, *218*, 179–194, doi:10.1144/GSL.SP.2005.248.01.10.

Raiswell, R., R. Newton, S. H. Bottrell, P. M. Coburn, D. E. G. Briggs, D. P. G. Bond, and S. W. Poulton (2008), Turbidite depositional influences on the diagenesis of Beecher's Trilobite Bed and the Hunsruck Slate; sites of soft tissue pyritization, *Am. J. Sci.*, *308*(2), 105–129, doi:10.2475/02.2008.01.

Schlanger, S. O., and H. C. Jenkyns (1976), Cretaceous anoxic events: Causes and consequences, *Geol. Mijnbouw*, *55*, 179–184.

Schlanger, S. O., M. A. Arthur, H. C. Jenkyns, and P. A. Scholle (1987), The Cenomanian-Turonian Oceanic Anoxic Event, I. Stratigraphy and distribution of organic carbon-rich beds and the marine $\delta^{13}C$ excursion, in *Marine Petroleum Source Rocks*, edited by J. Brooks and A. J. Fleet, *Geol. Soc. London Spec. Publ.*, *26*, 371–399, doi:10.1144/GSL.SP.1987.026.01.24.

Scholle, P. A., and M. A. Arthur (1980), Carbon isotope fluctuations in Cretaceous pelagic limestones; potential stratigraphic and petroleum exploration tool, *AAPG Bull.*, *64*(1), 67–87.

Scott, C., and T. W. Lyons (2012), Contrasting molybdenum cycling and isotopic properties in euxinic versus non-euxinic sediments and sedimentary rocks: Refining the paleoproxies, *Chem. Geol.*, doi:10.1016/j.chemgeo.2012.05.012, in press.

Scott, C., T. W. Lyons, A. Bekker, Y. Shen, S. W. Poulton, X. Chu, and A. D. Anbar (2008), Tracing the stepwise oxygenation of the Proterozoic ocean, *Nature*, *452*(7186), 456–459, doi:10.1038/nature06811.

Severmann, S., C. M. Johnson, B. L. Beard, C. R. German, H. N. Edmonds, H. Chiba, and D. R. H. Green (2004), The effect of plume processes on the Fe isotope composition of hydrothermally derived Fe in the deep ocean as inferred from the Rainbow vent site, Mid-Atlantic Ridge, 36°14′N, *Earth Planet. Sci. Lett.*, *225*(1–2), 63–76, doi:10.1016/j.epsl.2004.06.001.

Severmann, S., C. M. Johnson, B. L. Beard, and J. McManus (2006), The effect of early diagenesis on the Fe isotope compositions of porewaters and authigenic minerals in continental margin sediments, *Geochim. Cosmochim. Acta*, *70*(8), 2006–2022, doi:10.1016/j.gca.2006.01.007.

Severmann, S., T. W. Lyons, A. Anbar, J. McManus, and G. Gordon (2008), Modern iron isotope perspective on the benthic iron shuttle and the redox evolution of ancient oceans, *Geology*, *36*(6), 487–490, doi:10.1130/G24670A.1.

Severmann, S., J. McManus, W. M. Berelson, and D. E. Hammond (2010), The continental shelf benthic iron flux and its isotope composition, *Geochim. Cosmochim. Acta*, *74*(14), 3984–4004, doi:10.1016/j.gca.2010.04.022.

Sharma, M., M. Polizzotto, and A. D. Anbar (2001), Iron isotopes in hot springs along the Juan de Fuca Ridge, *Earth Planet. Sci. Lett.*, *194*(1–2), 39–51, doi:10.1016/S0012-821X(01)00538-6.

Shipboard Scientific Party (2004), Leg 207 summary, *Proc. Ocean Drill. Program Initial Rep.*, *207*, 89 pp., doi:10.2973/odp.proc.ir.207.101.2004.

Sinninghe Damsté, J. S., and J. Köster (1998), A euxinic southern North Atlantic Ocean during the Cenomanian/Turonian oceanic anoxic event,

Earth Planet. Sci. Lett., *158*(3–4), 165–173, doi:10.1016/S0012-821X(98)00052-1.

Sinton, C. W., and R. A. Duncan (1997), Potential links between ocean plateau volcanism and global ocean anoxia at the Cenomanian-Turonian boundary, *Econ. Geol.*, *92*(7–8), 836–842, doi:10.2113/gsecongeo.92.7-8.836.

Skulan, J. L., B. L. Beard, and C. M. Johnson (2002), Kinetic and equilibrium Fe isotope fractionation between aqueous Fe(III) and hematite, *Geochim. Cosmochim. Acta*, *66*(17), 2995–3015, doi:10.1016/S0016-7037(02)00902-X.

Snow, L. J., R. A. Duncan, and T. J. Bralower (2005), Trace element abundances in the Rock Canyon Anticline, Pueblo, Colorado, marine sedimentary section and their relationship to Caribbean plateau construction and oxygen anoxic event 2, *Paleoceanography*, *20*, PA3005, doi:10.1029/2004PA001093.

Stookey, L. L. (1970), Ferrozine—A new spectrophotometric reagent for iron, *Anal. Chem.*, *42*(7), 779–781, doi:10.1021/ac60289a016.

Taylor, S. R., and S. M. McLennan (1995), The Geochemical Evolution of the Continental Crust, *Rev. Geophys.*, *33*(2), 241–265, doi:10.1029/95RG00262.

Thurow, J. (1988), Cretaceous radiolarians of the North Atlantic Ocean: ODP Leg 103(Sites 638, 640, and 641) and DSDP Legs 93(Site 603) and 47B (Site 398), *Proc. Ocean Drill. Program Sci. Results*, *103*, 379–418, doi:10.2973/odp.proc.sr.103.148.1988.

Trabucho Alexandre, J., E. Tuenter, G. A. Henstra, K. J. van der Zwan, R. S. W. van de Wal, H. A. Dijkstra, and P. L. de Boer (2010), The mid-Cretaceous North Atlantic nutrient trap: Black shales and OAEs, *Paleoceanography*, *25*, PA4201, doi:10.1029/2010PA001925.

Tsikos, H., et al. (2004), Carbon-isotope stratigraphy recorded by the Cenomanian–Turonian Oceanic Anoxic Event: Correlation and implications based on three key localities, *J. Geol. Soc.*, *161*(4), 711–719, doi:10.1144/0016-764903-077.

Turekian, K. K., and K. H. Wedepohl (1961), Distribution of the elements in some major units of the Earth's crust, *Geol. Soc. Am. Bull.*, *72*(2), 175–192, doi:10.1130/0016-7606(1961)72[175:DOTEIS]2.0.CO;2.

Turgeon, S. C., and R. A. Creaser (2008), Cretaceous oceanic anoxic event 2 triggered by a massive magmatic episode, *Nature*, *454*(7202), 323–326, doi:10.1038/nature07076.

van Bentum, E. C., A. Hetzel, H.-J. Brumsack, A. Forster, G.-J. Reichart, and J. S. Sinninghe Damsté (2009), Reconstruction of water column anoxia in the equatorial Atlantic during the Cenomania-Turonian oceanic anoxic event using biomarker and trace metal proxies, *Palaeogeogr. Palaeoclimatol. Palaeoecol.*, *280*(3–4), 489–498, doi:10.1016/j.palaeo.2009.07.003.

van Hinte, J. E., et al. (1987), *Initial Reports of the Deep Sea Drilling Project*, vol. 93, 1423 pp., U.S. Gov. Print. Off., Washington, D. C.

Viollier, E., P. W. Inglett, K. Hunter, A. N. Roychoudhury, and P. Van Cappellen (2000), The ferrozine method revisited: Fe(II)/Fe(III) determination in natural waters, *Appl. Geochem.*, *15*(6), 785–790, doi:10.1016/S0883-2927(99)00097-9.

Wijsman, J. W. M., J. J. Middelburg, and C. H. R. Heip (2001), Reactive iron in Black Sea Sediments: Implications for iron cycling, *Mar. Geol.*, *172*(3–4), 167–180, doi:10.1016/S0025-3227(00)00122-5.